

# NJC

Accepted Manuscript



This is an *Accepted Manuscript*, which has been through the Royal Society of Chemistry peer review process and has been accepted for publication.

*Accepted Manuscripts* are published online shortly after acceptance, before technical editing, formatting and proof reading. Using this free service, authors can make their results available to the community, in citable form, before we publish the edited article. We will replace this *Accepted Manuscript* with the edited and formatted *Advance Article* as soon as it is available.

You can find more information about *Accepted Manuscripts* in the [Information for Authors](#).

Please note that technical editing may introduce minor changes to the text and/or graphics, which may alter content. The journal's standard [Terms & Conditions](#) and the [Ethical guidelines](#) still apply. In no event shall the Royal Society of Chemistry be held responsible for any errors or omissions in this *Accepted Manuscript* or any consequences arising from the use of any information it contains.



[www.rsc.org/njc](http://www.rsc.org/njc)

## COMMUNICATION

## Improved light absorption and photocatalytic activity of Zn,N-TiO<sub>2-x</sub> rich in oxygen vacancies obtained by nitridation and hydrogenation

Cite this: DOI: 10.1039/x0xx00000x

Received 00th January 2012,  
Accepted 00th January 2012

Yidong Hu, Gang Chen,\* Chunmei Li, Yaoguang Yu, Jingxue Sun and Hongjun Dong

DOI: 10.1039/x0xx00000x

www.rsc.org/

**Zn,N-codoped TiO<sub>2</sub> rich in oxygen vacancies (Zn,N-TiO<sub>2-x</sub>) was synthesized by nitridation and hydrogenation of zinc titanium precursor for the first time, which expands visible light harvest region and improves photocatalytic activity than the sample (Zn,N-TiO<sub>2</sub>) without hydrogenation.**

In previous decades, semiconductor photocatalysis has been widely investigated to decompose industrial wastewaters and organic dyes.<sup>1-4</sup> Plenty of efforts have been pursued to explore high efficiency photocatalysts for degradation of environmental pollutants.<sup>5-8</sup> As we known, much effort has been focused on TiO<sub>2</sub> photocatalyst materials because of its special photoelectric properties, low-cost, high efficiency and permanent photo-stability.<sup>9</sup> However, the wide band-gap of TiO<sub>2</sub> makes it be excited by the ultraviolet light ( $\lambda < 400$  nm) only.<sup>10</sup> Thus, in order to expand the range of visible light absorption regions, multitudinous strategies have been carried out to narrow the band gap.<sup>11, 12</sup> It was reported that doping some transition-metal (Fe,<sup>13</sup> Nb,<sup>14</sup> Zn,<sup>15</sup> Cr,<sup>16</sup> etc.) or nonmetal (N,<sup>17-19</sup> B,<sup>20</sup> F,<sup>21, 22</sup> S,<sup>23</sup> etc.) into TiO<sub>2</sub> can narrow the band gap effectively to promote the absorption range toward the visible light. Especially, TiO<sub>2</sub> co-doped with transition metal and nonmetal element has attracted much attention because of its outstanding optical and electronic properties.<sup>24, 25</sup> In addition, introducing crystal defects into TiO<sub>2</sub> by hydrogenation has been developed to be an effective modification approach in recent years.<sup>26</sup> It was demonstrated that oxygen vacancy defects on the TiO<sub>2</sub> surface can narrow the band gap to expand the light harvest region, thus improving the activity of photocatalysts.<sup>27, 28</sup>

In this study, we synthesized a Zn,N-TiO<sub>2-x</sub> photocatalyst fabricated by nitridation and hydrogenation of zinc titanium precursor. Especially, employing hydrogen treatment process, we obtain the oxygen vacancies with high concentrations in Zn,N-TiO<sub>2-x</sub> to further enhance light absorption ability. The as-prepared sample rich in oxygen vacancies displays superior photocatalytic degradation activity compared with the Zn,N-TiO<sub>2</sub> sample without hydrogenation.

The morphology of Zn,N-TiO<sub>2-x</sub> was depicted in the TEM image. As shown in Fig. 1a, the Zn,N-TiO<sub>2-x</sub> sample was composed of numerous nanoparticles with the size less than 50 nm. The size of the nanoparticles became larger with hydrogen treatment as can be

seen by the TEM images in Fig. S1. The nanoparticles exhibited slight agglomeration phenomenon, which may be due to the result of high-temperature calcination. In addition, the diffraction rings in SAED pattern (insert of Fig. 1a) revealed that the sample had polycrystalline characteristic. The HRTEM image in Fig. 1b indicated that there were two kinds of lattice fringes with the d-spacing of 0.245 nm and 0.351 nm, corresponding to the anatase (101) and rutile (101) planes, respectively. The results indicated the as-prepared sample was a mixture of anatase with rutile. It was beneficial to facilitate the separation of photoexcited charge carriers for enhancing the photocatalytic performance.<sup>29</sup>

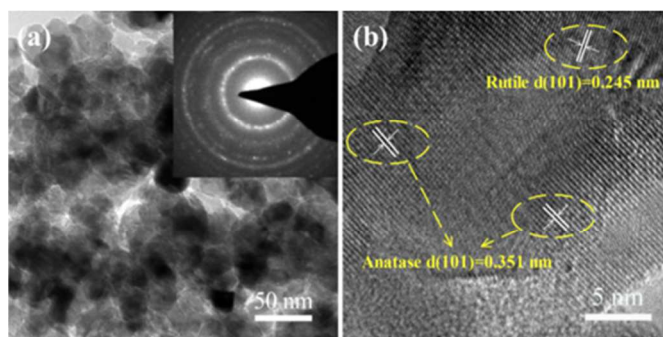


Fig. 1 TEM image (a) SAED pattern (the inset of a) and HRTEM image (b) of Zn,N-TiO<sub>2-x</sub> sample.

The strong sharp diffraction peaks suggested the samples were well-crystallized. Both of the samples exhibited the similar patterns which consisted well with the standard anatase and rutile. It suggested the as-prepared sample was composed of anatase and rutile TiO<sub>2</sub>, which was in good agreement with the HRTEM analysis. Moreover, the crystal structure and phase composition did not change after calcination under H<sub>2</sub> flow.

The light absorption properties of Zn,N-TiO<sub>2</sub> and Zn,N-TiO<sub>2-x</sub> samples was measured by UV-vis DRS. As shown in Fig. 2b, their steep absorption edge indicated the light absorptions derived from the band-gap transition.<sup>30</sup> The Zn,N-TiO<sub>2</sub> sample showed an absorption edge around 423 nm, the obviously red-shift of which may be attributed to the co-doping of zinc and nitrogen. It was crucial that the absorption edge of Zn,N-TiO<sub>2-x</sub> sample reached to

about 440 nm, which further red-shifted 17 nm compared with that of  $\text{Zn}_x\text{N-TiO}_2$ . The absorption band of  $\text{Zn}_x\text{N-TiO}_{2-x}$  extending dramatically toward to the visible light region results from production of the high concentration of oxygen vacancies by high-temperature hydrogenation. As a result, considering the sufficient use of solar light, it was believed that the  $\text{Zn}_x\text{N-TiO}_{2-x}$  sample can utilize the visible light more efficiently than  $\text{Zn}_x\text{N-TiO}_2$  in improving photocatalytic activity.

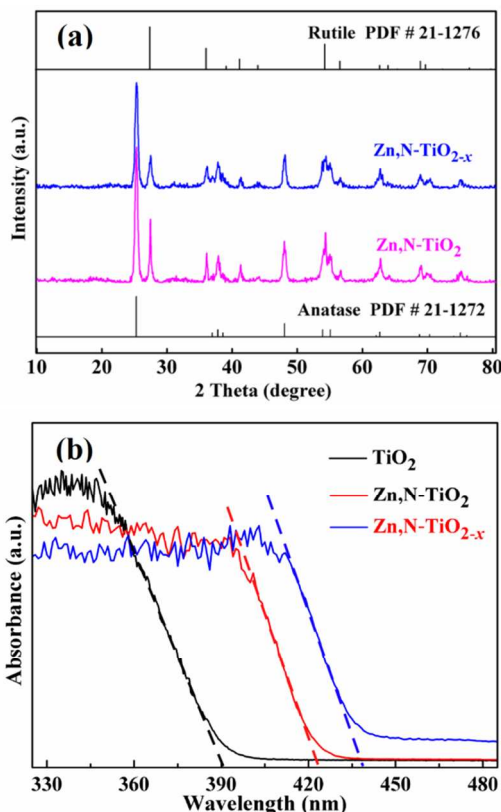


Fig. 2 (a) XRD patterns of the  $\text{Zn}_x\text{N-TiO}_2$  and  $\text{Zn}_x\text{N-TiO}_{2-x}$  samples and (b) UV-vis DRS of the  $\text{TiO}_2$ ,  $\text{Zn}_x\text{N-TiO}_2$  and  $\text{Zn}_x\text{N-TiO}_{2-x}$  samples.

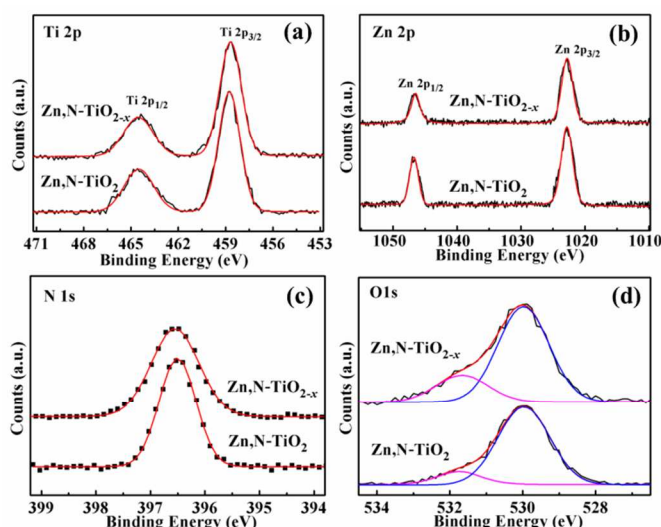


Fig. 3 High-resolution XPS spectra of the  $\text{Zn}_x\text{N-TiO}_2$  and  $\text{Zn}_x\text{N-TiO}_{2-x}$  samples: (a) Ti 2p, (b) Zn 2p, (c) N 1s and (d) O 1s.

XPS measurements were carried out to investigate the chemical compositions and surface valence states of  $\text{Zn}_x\text{N-TiO}_2$  and  $\text{Zn}_x\text{N-TiO}_{2-x}$  samples. Fig. 3 showed the high-resolution XPS spectra over the O1s, Ti 2p, Zn 2p, and N 1s peak regions. Two peaks at 458.7 eV and 464.5 eV for both sample belonged to the Ti  $2p_{3/2}$  and  $2p_{1/2}$  states, respectively (Fig. 3a), which matched very well with chemical states of  $\text{Ti}^{4+}$  in  $\text{TiO}_2$ .<sup>31</sup> In addition, as shown in Fig. 3b, the peaks of Zn  $2p_{3/2}$  and Zn  $2p_{1/2}$  states were observed at 1022.8 eV (1022.7 eV) and 1046.8 eV (1046.6 eV) in the XPS spectra for  $\text{Zn}_x\text{N-TiO}_2$  ( $\text{Zn}_x\text{N-TiO}_{2-x}$ ), respectively. Meanwhile, the N 1s feature peak arose from Ti-N bonds was observed at 396.6 eV for both samples (Fig. 3c), which had been reported in the previously research results.<sup>32,33</sup> The evidences above indicated Zn and N elements were doped into the  $\text{TiO}_2$  sample. Most importantly, the XPS spectrum of the O 1s region in Fig. 3d can be further divided into two components, in which the O1s peak at 530.0 eV was assigned to lattice oxygen while the small shoulder peaks at 531.7 eV was assigned to oxygen vacancies.<sup>34</sup> It was interesting that the intensity of the shoulder peak in the  $\text{Zn}_x\text{N-TiO}_{2-x}$  sample was obviously stronger than that in  $\text{Zn}_x\text{N-TiO}_2$ . According to the peak areas, further analysis revealed that the oxygen vacancies concentration accounted for 12.1 % for  $\text{Zn}_x\text{N-TiO}_2$ , and 23.6 % for  $\text{Zn}_x\text{N-TiO}_{2-x}$ .<sup>34</sup> Furthermore, the oxygen vacancy of  $\text{Zn}_x\text{N-TiO}_{2-x}$  was supported by Raman spectra (Fig. S2). The Raman Eg  $144\text{ cm}^{-1}$  mode of  $\text{Zn}_x\text{N-TiO}_{2-x}$  experiences a strong blue shift accompanied by peak broadening, compared with  $\text{Zn}_x\text{N-TiO}_2$ . It was ascribed to the oxygen nonstoichiometry.<sup>35, 36</sup> The higher concentration of oxygen vacancies for  $\text{Zn}_x\text{N-TiO}_{2-x}$  sample was an important factor in improving its light harvest ability.

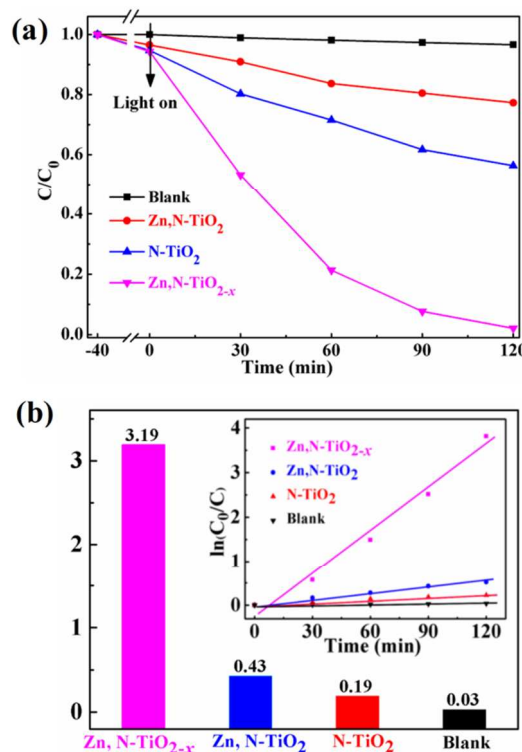


Fig. 4 (a) Dynamic curves of RhB photodegradation over  $\text{N-TiO}_2$ ,  $\text{Zn}_x\text{N-TiO}_2$  and  $\text{Zn}_x\text{N-TiO}_{2-x}$  under visible light irradiation and (b) RhB decomposition rate constant, and pseudo-first-order kinetic rate plots (the insert of b).

The photocatalytic activity of  $\text{N-TiO}_2$  (P25 heated at  $800\text{ }^\circ\text{C}$  for 5 h under  $\text{NH}_3$ ),  $\text{Zn}_x\text{N-TiO}_{2-x}$  and  $\text{Zn}_x\text{N-TiO}_2$  were evaluated by photodegradation of RhB dye in aqueous solution under visible light

irradiation ( $\lambda > 400$  nm). Fig. 4a showed the kinetic curves of RhB solutions degradation. Zn,N-TiO<sub>2-x</sub> displayed the slightly higher RhB absorption ability than N-TiO<sub>2</sub> and Zn,N-TiO<sub>2</sub> for 40 min in dark. The photolysis of RhB was negligible without photocatalyst under visible light irradiation. N-TiO<sub>2</sub> and Zn,N-TiO<sub>2</sub> samples had the slight removing capability for decomposing RhB and their decomposed about 16% and 25% within 120 min, respectively. It was worth noting that Zn,N-TiO<sub>2-x</sub> can completely remove RhB under the same conditions, demonstrating it had higher photocatalytic activity than that of N-TiO<sub>2</sub> and Zn,N-TiO<sub>2</sub>. These results proved that introducing high concentration oxygen vacancies was an effectively technique to improve photocatalytic activity of Zn,N-TiO<sub>2-x</sub>. Moreover, kinetic curves of RhB photocatalytic degradation based on the data plots was shown in the insert of Fig. 4b. The plots of  $\ln(C_0/C)$  vs time were transformed. The linear curve indicated the photocatalytic degradation of RhB matched with pseudo-first-order reaction.<sup>37</sup> The reaction rate constant  $k$  of RhB photodegradation over the Zn,N-TiO<sub>2-x</sub> sample was 0.0319 min<sup>-1</sup>, which reached to 7.4, 16.8 and 106.3 times as much as that of Zn,N-TiO<sub>2</sub> (0.0043 min<sup>-1</sup>), N-TiO<sub>2</sub> (0.0019 min<sup>-1</sup>) and blank (0.0003 min<sup>-1</sup>), respectively, indicating an outstanding photocatalytic performance of the sample Zn,N-TiO<sub>2-x</sub>. Moreover, for further verifying the photocatalytic ability of Zn,N-TiO<sub>2-x</sub> sample, the photocatalytic degradation of MO was carried out. After visible light irradiation for 120 min, the photodegradation efficiencies of MO over Zn,N-TiO<sub>2-x</sub> was about 49% (Fig. S3). The above results indicated that Zn,N-TiO<sub>2-x</sub> sample was a kind of outstanding photocatalyst.

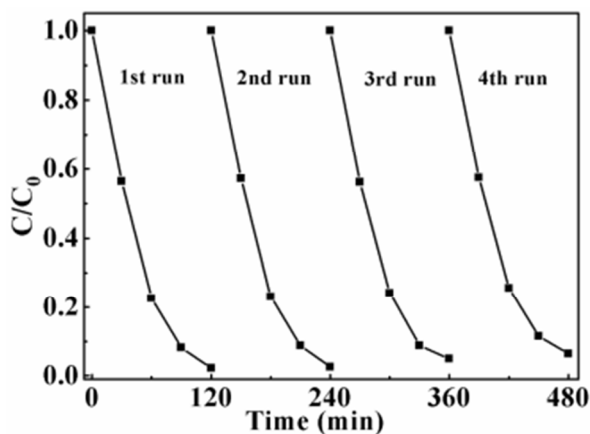


Fig. 5 Cycling runs of RhB degradation over Zn,N-TiO<sub>2-x</sub>.

Furthermore, the stability and reusability were important factors for photocatalyst evaluation. The cycle degradation experiments of RhB solutions were carried out (Fig. 5). After every 120 min photocatalytic reaction, the photocatalyst was separated from the reaction solution by centrifugation and then put into the RhB solution in the reactor to perform photocatalytic reaction. As shown in Fig. 5, after four cycle operations, the photocatalytic activity of Zn,N-TiO<sub>2-x</sub> sample did not show distinct loss. So the as-prepared Zn,N-TiO<sub>2-x</sub> had outstanding stability and durability.

All of above demonstrate N doping was an important factor for the photocatalytic activity of TiO<sub>2</sub>. Because N p states contribute to the band gap narrowed by effective mixing with O 2p for increasing visible light absorption.<sup>38</sup> Zn and N co-doped TiO<sub>2</sub> has superior photocatalytic activities due to its high transparency and small lattice mismatch upon doping compared with those of N doped TiO<sub>2</sub>.<sup>39</sup> In addition, TiO<sub>2</sub> with oxygen vacancies were found to be efficient for photodegradation of RhB under visible light irradiation (Fig. S4). Moreover, Zn,N-TiO<sub>2-x</sub> sample still possess high photocatalytic activity under light source ( $\lambda > 420$ nm, Fig. S5). The high

photocatalytic activity can be ascribed to the synergistic effect of oxygen vacancies, Zn doping, N doping and efficient visible light absorption by the Zn,N-TiO<sub>2-x</sub> samples. Additionally, the PL emission peaks of two samples were located at 450 nm (Fig. S6). The weaker PL intensity of Zn,N-TiO<sub>2-x</sub> verify it has better separation efficiency of photo generated charge carriers.

To further investigate the effects of photodegradation mechanism of dyes, a typical experiments was performed (Fig. S7). The degradation of RhB over Zn,N-TiO<sub>2-x</sub> under a monochromatic wavelengths at 550 nm ( $\Delta\lambda = \pm 15$  nm) was carried out to ascertain the degradation pattern. The result shows that approximately 8% of RhB was degraded within 10 h, indicating that the effect of dye sensitization was negligible.<sup>40,41</sup> Therefore, the photodegradation of RhB was ascribed to self-oxidation of Zn,N-TiO<sub>2-x</sub>.

In summary, a new sensitive Zn,N-TiO<sub>2-x</sub> rich in oxygen vacancies was successfully prepared by nitridation and hydrogenation to zinc titanium precursors. Zn,N-TiO<sub>2-x</sub> exhibits improved visible light absorption ability and outstanding photocatalytic activity than that without hydrogenation. The synthetic strategy developed here provides insight to enhancing the catalytic activity of photocatalyst and will inspire the developing of new high efficient photocatalyst.

## Experimental

Preparation of Zn,N-TiO<sub>2-x</sub>: Anhydrous citric acid (10 mL) was dissolved in ethylene glycol, followed by adding tetrabutyl-titanate and zinc acetate with vigorous magnetic stirring at 80 °C for 1 h. The solution was heated at 140 °C for 20 h. Then, it was heated at 400 °C for several hours to burn out organics. Finally, the precursor powder was heated at 800 °C for 5 h under NH<sub>3</sub> flow, followed by calcination at 500 °C for 6 h in air to get Zn,N-TiO<sub>2</sub>. The resulting powders were maintained in H<sub>2</sub> atmosphere at 500 °C for 2 h. Zn,N-TiO<sub>2-x</sub> was obtained after washing and drying.

## Acknowledgements

This work was financially supported by projects of Natural Science Foundation of China (21271055, 21471040), the Fundamental Research Funds for the Central Universities (HIT. IBRSEM. A. 201410) and Open Project of State Key Laboratory of Urban Water Resource and Environment, Harbin Institute of Technology (QAK201304).

## Notes and references

<sup>a</sup> Department of Chemistry, Harbin Institute of Technology, Harbin 150001, P. R. China, E-mail: gchen@hit.edu.cn

- H. J. Dong, G. Chen, J. X. Sun and C. M. Li, *Appl. Catal. B: Environ.*, 2013, **134**, 46.
- L. L. Ruan, J. Q. Liu and Q. Zhou, *New J. Chem.*, 2014, **38**, 3022.
- C. M. Li, G. Chen, J. X. Sun and H. J. Dong, *Appl. Catal. B: Environ.*, 2014, **160**, 383.
- I. K. Konstantinou and T. A. Albanis, *Appl. Catal. B: Environ.*, 2004, **49**, 1.

- 5 M. Q. Yang, N. Zhang, M. Pagliaro and Y. J. Xu, *Chem. Soc. Rev.*, 2014, **43**, 8240.
- 6 N. Zhang, Y. H. Zhang and Y. J. Xu, *Nanoscale*, 2012, **4**, 5792.
- 7 C. Han, M. Q. Yang, B. Weng and Y. J. Xu, *Phys. Chem. Chem. Phys.*, 2014, **16**, 16891.
- 8 Y. H. Zhang, Z. R. Tang, X. Z. Fu and Y. J. Xu, *ACS Nano*, 2010, **4**, 7303.
- 9 R. Asahi, T. Morikawa, H. Irie and T. Ohwaki, *Chem. Rev.*, 2014, **114**, 9824.
- 10 G. Yang, Z. Jiang, H. Shi, T. Xiao and Z. Yan, *J. Mater. Chem.*, 2010, **20**, 5301.
- 11 G. Liu, L. C. Yin, J. Q. Wang, P. Niu and C. Zhen, *Environ. Eng. Sci.*, 2012, **5**, 9603.
- 12 X. D. Wang, K. Zhang, X. L. Guo, G. D. Shen and J. Y. Xiang, *New J. Chem.*, 2014, **38**, 6139.
- 13 K. C. Christoforidis, A. Iglesias-Juez, S. J. A. Figueroa and M. D. Michiel, *Catal. Sci. Technol.*, 2013, **3**, 626.
- 14 M. Yang, D. H. Kim, H. Jha, K. Lee, J. Paul and P. Schmuki, *Chem. Commun.*, 2011, **47**, 2032.
- 15 K. P. Wang and H. Teng, *Phys. Chem. Chem. Phys.*, 2009, **11**, 9489.
- 16 J. Y. Cao, Y. J. Zhang, L. Q. Liu and J. H. Ye, *Chem. Commun.*, 2013, **49**, 3440.
- 17 R. Asahi, T. Morikawa, T. Ohwaki, K. Aoki and Y. Taga, *Science*, 2001, **293**, 269.
- 18 X. D. Wang, K. Zhang, X. L. Guo, G. D. Shen and J. Y. Xiang, *New J. Chem.*, 2014, **38**, 6139.
- 19 G. D. Yang, Z. Jiang, H. H. Shi, T. C. Xiao and Z. F. Yan, *J. Mater. Chem.*, 2010, **20**, 5301.
- 20 J. G. Yu, P. Zhou and Q. Li, *Phys. Chem. Chem. Phys.*, 2013, **15**, 12040.
- 21 Y. C. Dong, M. Kapilashrami, Y. F. Zhang and J. H. Guo, *CrystEngComm*, 2013, **15**, 10657.
- 22 W. K. Ho, J. C. Yu and S. C. Lee, *Chem. Commun.*, 2006, 1115.
- 23 C. W. Dunnill, Z. A. Aiken, A. Kafizas, J. Pratten and M. Wilson, *J. Mater. Chem.*, 2009, **19**, 8747.
- 24 T. H. Kim, V. Rodríguez-González, G. Gyawali, S. H. Cho, T. Sekino and S. W. Lee, *Catal. Today*, 2013, **212**, 75.
- 25 S. B. Khan, M. M. Rahman, A. M. Asiri and H. M. Marwani, *New J. Chem.*, 2013, **37**, 2888.
- 26 X. B. Chen, L. Liu, Y. Y. Peter and S. S. Mao, *Science*, 2011, **331**, 746.
- 27 A. Naldoni, M. Allieta, S. Santangelo, M. Marelli and F. Fabbri, *J. Am. Chem. Soc.*, 2012, **134**, 7600.
- 28 X. Y. Pan, M. Q. Yang, X. Z. Fu, N. Zhang and Y. J. Xu, *Nanoscale*, 2013, **5**, 3601.
- 29 D. O. Scanlon, C. W. Dunnill, J. Buckeridge, S. A. Shevlin, A. J. Logsdail and S. M. Woodley, *Nat. Mater.*, 2013, **12**, 798.
- 30 A. Kudo, I. Tsuji and H. Kato, *Chem. Commun.*, 2002, 1958.
- 31 S. Hoang, S. P. Berglund, N. T. Hahn, A. J. Bard and C. B. Mullins, *J. Am. Chem. Soc.*, 2012, **134**, 3659.
- 32 P. Romero-Gomez, V. Rico, A. Borrás, A. Barranco, J. P. Espinos and J. Cotrino, *J. Phys. Chem. C.*, 2009, **113**, 13341.
- 33 Liu, Y., Chen, G., Zhou, C., Y. D. Hu and D. G. Fu, *J. Hazard. Mater.*, 2011, 190, 75.
- 34 J. P. Wang, Z. Y. Wang, B. B. Huang, Y. D. Ma, Y. Y. Liu and X. Y. Qin, *Appl. Mater. Interfaces*, 2012, **4**, 4024.
- 35 A. L. Bassi, D. Cattaneo, V. Russo, C. E. Bottani and E. Barborini, *J. Appl. Phys.*, 2005, **98**, 074305.
- 36 Z. Wang, C. Y. Yang, T. Q. Lin, H. Yin and P. Chen, *Energy Environ. Sci.*, 2013, **6**, 3007.
- 37 I. K. Konstantinou and T. A. Albanis, *Appl. Catal. B: Environ*, 2004, **49**, 1.
- 38 R. Asahi, T. Morikawa, H. Irie and T. Ohwaki, *Chem. Rev.*, 2014, **114**, 9824.
- 39 M. Thambidurai, J. Y. Kim, Y. J. Ko, H. J. Song and H. Shin, *Nanoscale*, 2014, **6**, 8585.
- 40 H. J. Dong, G. Chen, J. X. Sun, Y. J. Feng and C. M. Li, *Dalton Trans.*, 2014, **43**, 7282.
- 41 L. Yuan, M. Q. Yang and Y. J. Xu, *Nanoscale*, 2014, **6**, 6335.